

Classical predictability and coarse-grained evolution of the quantum baker's map

Artur Scherer, Andrei N. Soklakov, and Rüdiger Schack

Department of Mathematics, Royal Holloway,

University of London, Egham, Surrey TW20 0EX, UK

(Dated: July 18, 2018)

We investigate how classical predictability of the coarse-grained evolution of the quantum baker's map depends on the character of the coarse-graining. Our analysis extends earlier work by Brun and Hartle [Phys. Rev. D **60**, 123503 (1999)] to the case of a chaotic map. To quantify predictability, we compare the rate of entropy increase for a family of coarse-grainings in the decoherent histories formalism. We find that the rate of entropy increase is dominated by the number of scales characterising the coarse-graining.

I. INTRODUCTION

The concept of coarse-graining plays an important role in the emergence of classical evolution from the fundamental quantum-mechanical equations of motion [1, 2]. The form of the effective classical equations of motion is as much influenced by the character of the coarse-graining as by the fundamental quantum-mechanical equations of motion themselves. A systematic way to study coarse-grained quantum evolution is provided by the decoherent histories formalism [1, 3, 4, 5, 6]. Within this approach to quantum theory a quantum mechanical system is said to exhibit classical behaviour when histories with correlations in time that are implied by classical deterministic laws have high probability [1, 2].

Coarse-grained descriptions are also used in classical physics to reduce the number of variables when the number of degrees of freedom is large. This leads to effective equations of motion for the coarse-grained variables. The character of the coarse-graining is important here. Although a given physical system may be described by many alternative sets of coarse-grained variables, some coarse-grained descriptions are more useful for prediction than others. For a practical set of coarse-grained variables, the observables of interest should be simple and slowly varying functions.

In quantum theory, the nonuniqueness of the coarse-graining procedure motivates this question: what distinguishes coarse-grainings leading to predictable, deterministic effective classical evolution from other coarse-grainings? In general, arbitrarily many sets of alternative coarse-grained histories decohere and so can be assigned probabilities. Moreover, two such decoherent sets of histories are in general mutually incompatible. Which of these many possible coarse-grainings lead to predictable evolution of the coarse-grained variables, i.e., useful regularities in time governed by effective, phenomenological equations of motion?

These questions have been addressed by Brun and Hartle in Ref. [2], where they investigate the origin of classical predictability by considering the simplest linear system with a continuum description—the linear one-dimensional harmonic chain regarded as a closed quantum mechanical system. In their analysis a chain of \mathcal{N} atoms is divided up into groups of N atoms each. Each such group is then itself further subdivided into N/d equally spaced clumps of d atoms each, with a distance between clumps of $(\mathcal{N}/N) \cdot d$. A family of coarse-grained descriptions is introduced by restricting attention to the average positions of the atoms in a group, which are regarded as the relevant variables defining the system under consideration, and ignoring the internal coordinates within each group, which are regarded as the “environment”. In the case $d = N$ the N atoms of each group are all neighbours. The corresponding coarse-grained description is therefore entirely local. As d decreases from N to 1 the coarse-grained description becomes more and more nonlocal. In the case $d = 1$ the N atoms of each group are dispersed over the whole chain. Brun and Hartle analyse how decoherence, noise and computational complexity of the coarse-grained evolution depends on the nonlocality parameter d and thus show that local coarse-grainings are characterised by a higher degree of classical predictability.

The dynamical system studied by Brun and Hartle is linear. In this paper we analyse classical predictability for a family of coarse grainings for a *nonlinear* chaotic map, the quantum baker’s map [7, 8]. To quantify predictability, we compute the entropy increase for the evolution: the greater the rate of entropy increase, the less predictable is the evolution. We consider a family of hierarchical multi-scale coarse grainings and show that predictability decreases as the number of scales characterising the coarse-graining increases.

The paper is organised as follows. We start with a short introduction to the quantum baker’s map (Sec. II A) and the decoherent histories formalism (Sec. II B). We then introduce the family of coarse grainings (Sec. III A), describe how the rate of entropy increase depends

on the coarse-graining (Sec. III B), and finally present detailed derivations of our results (Sec. III C).

II. BACKGROUND

A. Quantum baker's map

The quantum baker's map [7, 8] is a prototypical quantum map invented for the theoretical investigation of quantum chaos. It was introduced as a quantised version of the classical baker's transformation [9]. There is, however, no unique quantisation procedure [10]. The original definition of the map [7, 8] is based on Weyl's quantisation [11] of the unit square. In [12] a class of quantum baker's maps has been defined by exploiting formal similarities between the symbolic dynamics [13] for the classical baker's map on the one hand and the dynamics of strings of quantum bits (qubits) on the other hand. These maps admit a symbolic description in terms of shifts on strings of qubits similar to classical symbolic dynamics [13]. Their symbolic description has been further developed in [14].

Let us give a short introduction following [12]. Quantum baker's maps are defined on the D -dimensional Hilbert space of the quantised unit square [11]. For consistency of units, we let the quantum scale on "phase space" be $2\pi\hbar = 1/D$. Following Ref. [8], we choose half-integer eigenvalues $q_j = (j + \frac{1}{2})/D$, $j = 0, \dots, D-1$, and $p_k = (k + \frac{1}{2})/D$, $k = 0, \dots, D-1$, of the discrete "position" and "momentum" operators \hat{q} and \hat{p} , respectively, corresponding to antiperiodic boundary conditions. We further assume that $D = 2^N$, which is the dimension of the Hilbert space of N qubits.

The $D = 2^N$ dimensional Hilbert space modelling the unit square can be identified with the product space of N qubits via

$$|q_j\rangle = |\xi_1\rangle \otimes |\xi_2\rangle \otimes \dots \otimes |\xi_N\rangle, \quad (2.1)$$

where $j = \sum_{l=1}^N \xi_l 2^{N-l}$, $\xi_l \in \{0, 1\}$, and where each qubit has basis states $|0\rangle$ and $|1\rangle$. We can write q_j as a binary fraction, $q_j = 0.\xi_1\xi_2\dots\xi_N1$. Let us define the notation

$$|.\xi_1\xi_2\dots\xi_N\rangle = e^{i\pi/2}|q_j\rangle; \quad (2.2)$$

see Ref. [12] for the reason for the phase factor $e^{i\pi/2}$. Momentum and position eigenstates are related through the quantum Fourier transform operator \hat{F} [8], i.e., $\hat{F}|q_k\rangle = |p_k\rangle$.

By applying the Fourier transform operator to the n rightmost bits of the position eigenstate $|\xi_{n+1} \dots \xi_N \xi_n \dots \xi_1\rangle$, one obtains the family of states [12]

$$\begin{aligned}
|\xi_1 \dots \xi_n \cdot \xi_{n+1} \dots \xi_N\rangle &\equiv 2^{-n/2} e^{i\pi(0.\xi_n \dots \xi_1 1)} |\xi_{n+1}\rangle \otimes \dots \otimes |\xi_N\rangle \otimes \\
&(|0\rangle + e^{2\pi i(0.\xi_1 1)} |1\rangle) \otimes (|0\rangle + e^{2\pi i(0.\xi_2 \xi_1 1)} |1\rangle) \otimes \\
&(|0\rangle + e^{2\pi i(0.\xi_3 \xi_2 \xi_1 1)} |1\rangle) \otimes \dots \otimes \\
&(|0\rangle + e^{2\pi i(0.\xi_n \dots \xi_1 1)} |1\rangle), \tag{2.3}
\end{aligned}$$

where $1 \leq n \leq N - 1$. For fixed values of n and N we will use the notation

$$|\xi_1 \dots \xi_N\rangle_n \equiv |\xi_1 \dots \xi_n \cdot \xi_{n+1} \dots \xi_N\rangle. \tag{2.4}$$

These states form an orthonormal basis of the Hilbert space. The state (2.3) is localised in both position and momentum: it is strictly localised within a position region of width $1/2^{N-n}$, centred at position $q = 0.\xi_{n+1} \dots \xi_N 1$, and it is approximately localised within a momentum region of width $1/2^n$, centred at momentum $p = 0.\xi_n \dots \xi_1 1$.

For each fixed n , $0 \leq n \leq N - 1$, the quantum baker's map B_n is defined by

$$B_n |\xi_1 \dots \xi_n \cdot \xi_{n+1} \dots \xi_N\rangle = |\xi_1 \dots \xi_{n+1} \cdot \xi_{n+2} \dots \xi_N\rangle, \tag{2.5}$$

i.e.

$$B_n |\xi_1 \dots \xi_N\rangle_n = |\xi_1 \dots \xi_N\rangle_{n+1}. \tag{2.6}$$

The action of the map B_n on the basis states (2.3) is thus given by a shift of the dot by one position. In phase-space language, the map \hat{B}_n takes a state localised at $(q, p) = (0.\xi_{n+1} \dots \xi_N 1, 0.\xi_n \dots \xi_1 1)$ to a state localised at $(q', p') = (0.\xi_{n+2} \dots \xi_N 1, 0.\xi_{n+1} \dots \xi_1 1)$, while it stretches the state by a factor of two in the q direction and squeezes it by a factor of two in the p direction. For $n = N - 1$, the map is the original quantum baker's map as defined in Ref. [8].

For the sake of clarity, it will be convenient to simplify our notation slightly. Throughout the paper n and N are fixed. So we may omit the index n and denote the quantum baker's map simply by B , always keeping in mind that we are dealing with the special baker's map B_n for the given value of n .

B. Decoherent histories formalism

The decoherent histories formalism [1, 3, 4, 5, 6] provides a framework for investigating classicality in quantum theory [1, 6]. The formalism assigns probabilities to quantum histories, i.e. ordered sequences of quantum-mechanical “propositions”. Mathematically, these propositions are represented by projectors. An exhaustive set of mutually exclusive propositions corresponds to a complete set of mutually orthogonal projectors. In this approach to quantum theory a quantum mechanical system is said to exhibit classical behaviour when the probability distribution over histories is strongly peaked about histories having correlations in time implied by classical deterministic laws [1, 2]. Due to quantum interference one cannot always assign probabilities to a set of histories in a consistent way. For this to be possible, the set of histories must be decoherent. Decoherence of histories is therefore a prerequisite for classical behaviour. In general, only coarse-grained sets of histories are decoherent.

For our purpose it will be sufficient to consider a slightly simplified version of the general decoherent histories framework, tailored to a system dynamics induced by a fixed unitary quantum map U and restricted to the special but natural case, in which histories are constructed from a fixed exhaustive set of mutually exclusive propositions.

A *projective partition* of a Hilbert space \mathcal{H} is a complete set of mutually orthogonal projection operators $\{P_\mu\}$ on \mathcal{H} , i.e., $P_\mu P_{\mu'} = \delta_{\mu\mu'} P_\mu$ and $\sum_\mu P_\mu = \mathbb{1}_{\mathcal{H}}$, where $\mathbb{1}_{\mathcal{H}}$ denotes the unit operator on \mathcal{H} . A projective partition is *fine-grained* if all projectors are one-dimensional, i.e., $\forall \mu \text{ rank}(P_\mu) = \dim(\text{supp}(P_\mu)) = 1$ [20], and *coarse-grained* otherwise.

Given a projective partition $\{P_\mu\}$ of a Hilbert space \mathcal{H} , a string of length k of projectors $P_\alpha \in \{P_\mu\}$ defines a history of length k :

$$h_\alpha \equiv (P_{\alpha_1}, P_{\alpha_2}, \dots, P_{\alpha_k}) , \quad (2.7)$$

where $\alpha \equiv \alpha_1 \alpha_2 \dots \alpha_k$. The set of all such histories, $\mathbb{H}[\{P_\mu\}; k] \equiv \{h_\alpha : h_\alpha \in \{P_\mu\}^k\}$, forms the exhaustive set of mutually exclusive histories of length k . Histories are ordered sequences of projection operators, corresponding to quantum-mechanical propositions. Note that we restrict attention to histories constructed from a fixed exhaustive set of mutually exclusive propositions: the projectors P_{α_j} within the sequences are all chosen from the same projective partition, for all times $j = 1, \dots, k$.

A set of histories $\mathbb{H}[\{P_\mu\}; k]$ is called *fine-grained* (*coarse-grained*) if it is constructed from a fine-grained (coarse-grained) projective partition. A single history $h_\alpha \in \mathbb{H}[\{P_\mu\}; k]$ is called *fine-grained*, if it is represented by a sequence of 1-dimensional projectors, and *coarse-grained* otherwise.

An initial state represented by a density operator ρ_0 on \mathcal{H} and a unitary dynamics generated by a unitary map $U : \mathcal{H} \rightarrow \mathcal{H}$ induce a probabilistic structure on the event algebra associated with $\mathbb{H}[\{P_\mu\}; k]$, if the following decoherence conditions are satisfied. These are given in terms of properties of the *decoherence functional* $\mathcal{D}_{U, \rho_0}[\cdot, \cdot]$ on $\mathbb{H}[\{P_\mu\}; k] \times \mathbb{H}[\{P_\mu\}; k]$, defined by

$$\mathcal{D}_{U, \rho_0} [h_\alpha, h_\beta] \equiv \text{Tr} \left[C_\alpha \rho C_\beta^\dagger \right], \quad (2.8)$$

where

$$\begin{aligned} C_\alpha \equiv C_{h_\alpha} &\equiv (U^\dagger P_{\alpha_k} U^k) (U^\dagger P_{\alpha_{k-1}} U^{k-1}) \dots (U^\dagger P_{\alpha_1} U) \\ &= U^\dagger P_{\alpha_k} U P_{\alpha_{k-1}} U \dots P_{\alpha_2} U P_{\alpha_1} U. \end{aligned} \quad (2.9)$$

The set of histories $\mathbb{H}[\{P_\mu\}; k]$ is said to be decoherent with respect to a given unitary map $U : \mathcal{H} \rightarrow \mathcal{H}$ and a given initial state ρ_0 , if

$$\mathcal{D}_{U, \rho_0} [h_\alpha, h_\beta] \propto \delta_{\alpha\beta} \equiv \prod_{j=1}^k \delta_{\alpha_j \beta_j} \quad (2.10)$$

for all $h_\alpha, h_\beta \in \mathbb{H}[\{P_\mu\}; k]$. If this decoherence condition is satisfied, the diagonal elements of the decoherence functional, $p[h_\alpha] = \mathcal{D}_{U, \rho_0} [h_\alpha, h_\alpha]$, can be interpreted as the probabilities of the histories. For a decoherent set of histories, the entropy, $H[\{h_\alpha\}]$, can be defined as follows [5, 15, 16]:

$$\begin{aligned} H[\{h_\alpha\}] &\equiv - \sum_{\alpha} p[h_\alpha] \log_2 p[h_\alpha] \\ &= - \sum_{\alpha} \mathcal{D}_{U, \rho_0} [h_\alpha, h_\alpha] \log_2 \left(\mathcal{D}_{U, \rho_0} [h_\alpha, h_\alpha] \right). \end{aligned} \quad (2.11)$$

III. PREDICTABILITY FOR DIFFERENT COARSE-GRAININGS OF THE QUANTUM BAKER'S MAP

This section is organised as follows. Subsection III A, which discusses coarse-grained descriptions of the quantum baker's map, contains two parts: part 1 introduces a family of

coarse-grained projective partitions of the Hilbert space, which are then used in part 2 to construct a class of coarse-grained sets of histories. Subsection III B summarises the main results of this paper, which are then derived and illustrated in detail in Subsection III C.

A. Coarse-grainings

1. Coarse-grained partitions

Let us first introduce two different types of coarse-grained projective partitions of the 2^N -dimensional Hilbert space modelling the unit square, which later will be regarded as special cases of a family of more general coarse-grained descriptions. We refer to the definitions and notations of Sec. II A. In particular we use the orthonormal basis (2.4) of the Hilbert space to construct the partitions.

For a fixed binary string $\mathbf{y} = y_1 \dots y_{N-l-r} \in \{0, 1\}^{N-l-r}$ we define the “local” projection operators by

$$P_{\mathbf{y}}^{(l,r)} \equiv \sum_{\substack{a_1, \dots, a_l \\ b_1, \dots, b_r}} |a_1 \dots a_l \mathbf{y} b_1 \dots b_r\rangle_n \langle a_1 \dots a_l \mathbf{y} b_1 \dots b_r| \equiv \sum_{\substack{\mathbf{a} \in \{0,1\}^l \\ \mathbf{b} \in \{0,1\}^r}} |\mathbf{a} \mathbf{y} \mathbf{b}\rangle_n \langle \mathbf{a} \mathbf{y} \mathbf{b}|, \quad (3.1)$$

and for fixed strings $\mathbf{y}^1 \in \{0, 1\}^{s_1}$ and $\mathbf{y}^2 \in \{0, 1\}^{s_2}$ we define the “nonlocal” projection operators by

$$\begin{aligned} P_{\mathbf{y}^1, \mathbf{y}^2}^{(l, m_l, m_r, r)} &\equiv \sum_{\mathbf{a} \in \{0,1\}^l} \sum_{\mathbf{b} \in \{0,1\}^r} \sum_{\xi \in \{0,1\}^{m_l+m_r}} |\mathbf{a} \mathbf{y}^1 \xi \mathbf{y}^2 \mathbf{b}\rangle_n \langle \mathbf{a} \mathbf{y}^1 \xi \mathbf{y}^2 \mathbf{b}| \quad (3.2) \\ &\equiv \sum_{\substack{a_1, \dots, a_l \\ b_1, \dots, b_r}} \sum_{\substack{\xi_1 \dots \xi_{m_l} \\ \xi_{m_l+1} \dots \xi_{m_l+m_r}}} |a_1 \dots a_l \mathbf{y}^1 \xi_1 \dots \xi_{m_l} \cdot \xi_{m_l+1} \dots \xi_{m_l+m_r} \mathbf{y}^2 b_1 \dots b_r\rangle \times \\ &\quad \langle a_1 \dots a_l \mathbf{y}^1 \xi_1 \dots \xi_{m_l} \cdot \xi_{m_l+1} \dots \xi_{m_l+m_r} \mathbf{y}^2 b_1 \dots b_r| \end{aligned}$$

What the terms “local” and “non-local” mean in this context, will be explained below. Throughout this paper, bold variables denote binary strings. Furthermore, lower indices label individual bits of a string, whereas upper indices will label different strings. It will be convenient to abbreviate a substring $\alpha_\kappa \dots \alpha_\sigma$ of a string $\boldsymbol{\alpha} = \alpha_1 \dots \alpha_\kappa \alpha_{\kappa+1} \dots \alpha_\sigma \alpha_{\sigma+1} \dots \alpha_\gamma$ by $\boldsymbol{\alpha}_{\kappa:\sigma}$. Concatenation of strings is defined in the usual way. Taking the just mentioned example we can, for instance, express the string $\boldsymbol{\alpha}$ as a concatenation of three substrings, $\boldsymbol{\alpha} = \boldsymbol{\alpha}_{1:\kappa-1} \boldsymbol{\alpha}_{\kappa:\sigma} \boldsymbol{\alpha}_{\sigma+1:\gamma}$. The length of a string $\boldsymbol{\alpha}$ will be denoted by $|\boldsymbol{\alpha}|$.

For simplicity, we will always assume in the following that $l < n$ and $r < N - n$ in the first case, and $l + s_1 \leq n$ and $r + s_2 \leq N - n$ in the second case. In both cases l and r acquire the specific meaning as the number of “momentum” and “position” bits ignored in the coarse-graining. In the second case, in addition m_l most significant momentum bits and m_r most significant position bits are coarse-grained over.

The operator $P_{\mathbf{y}}^{(l,r)}$ is a projector on a 2^{l+r} -dimensional subspace labelled by the string \mathbf{y} . The projector $P_{\mathbf{y}^1, \mathbf{y}^2}^{(l, m_l, m_r, r)}$ projects on a $2^{l+m_l+m_r+r}$ -dimensional subspace labelled by the pair of strings $(\mathbf{y}^1, \mathbf{y}^2)$. In both cases we are dealing with complete sets of mutually orthogonal projectors, i.e., with projective partitions, as

$$P_{\mathbf{y}}^{(l,r)} P_{\mathbf{y}'}^{(l,r)} = \delta_{\mathbf{y}, \mathbf{y}'} P_{\mathbf{y}}^{(l,r)} \quad \text{and} \quad \sum_{\mathbf{y}} P_{\mathbf{y}}^{(l,r)} = \mathbf{1}, \quad (3.3)$$

$$P_{\mathbf{y}^1, \mathbf{y}^2}^{(l, m_l, m_r, r)} P_{\mathbf{y}'^1, \mathbf{y}'^2}^{(l, m_l, m_r, r)} = \delta_{\mathbf{y}^1, \mathbf{y}'^1} \delta_{\mathbf{y}^2, \mathbf{y}'^2} P_{\mathbf{y}^1, \mathbf{y}^2}^{(l, m_l, m_r, r)} \quad \text{and} \quad \sum_{\mathbf{y}^1, \mathbf{y}^2} P_{\mathbf{y}^1, \mathbf{y}^2}^{(l, m_l, m_r, r)} = \mathbf{1}. \quad (3.4)$$

Let us explain what is meant by “local” and “nonlocal” regarding the just introduced projection operators. The projection operators $P_{\mathbf{y}}^{(l,r)}$ and $P_{\mathbf{y}^1, \mathbf{y}^2}^{(l, m_l, m_r, r)}$ project on subspaces of the Hilbert space associated with phase-space regions of the unit square in which the corresponding eigenstates with eigenvalue 1 are localised. In the case of the projectors $P_{\mathbf{y}}^{(l,r)}$ these regions are connected cells whose location within the unit square of the phase space is determined by the specified most significant position and momentum bits given by the binary string $\mathbf{y} = y_1 \dots y_{N-l-r}$. The size of these cells depends on the significance of the scales which are not resolved and therefore ignored, i.e. coarse-grained over. In the case of the projectors $P_{\mathbf{y}^1, \mathbf{y}^2}^{(l, m_l, m_r, r)}$, on the other hand, there is coarse-graining also at the most significant scales: a number of the most significant position and momentum bits are not specified. The associated phase space domains must therefore consist of disconnected parts spread over the whole unit square, the number depending on how many most significant position and momentum bits are coarse-grained over, i.e. on the parameter $m \equiv m_l + m_r$. For an illustration see Fig. 1.

We will also use the diagram notation for the introduced projectors:

$$P_{\mathbf{y}}^{(l,r)} \equiv (\underbrace{\square \square \dots \square}_l \mathbf{y} \underbrace{\square \square \dots \square}_r), \quad (3.5)$$

$$P_{\mathbf{y}^1, \mathbf{y}^2}^{(l, m_l, m_r, r)} \equiv (\underbrace{\square \square \dots \square}_l \mathbf{y}^1 \underbrace{\square \square \dots \square}_{m_l} \cdot \underbrace{\square \square \dots \square}_{m_r} \mathbf{y}^2 \underbrace{\square \square \dots \square}_r), \quad (3.6)$$

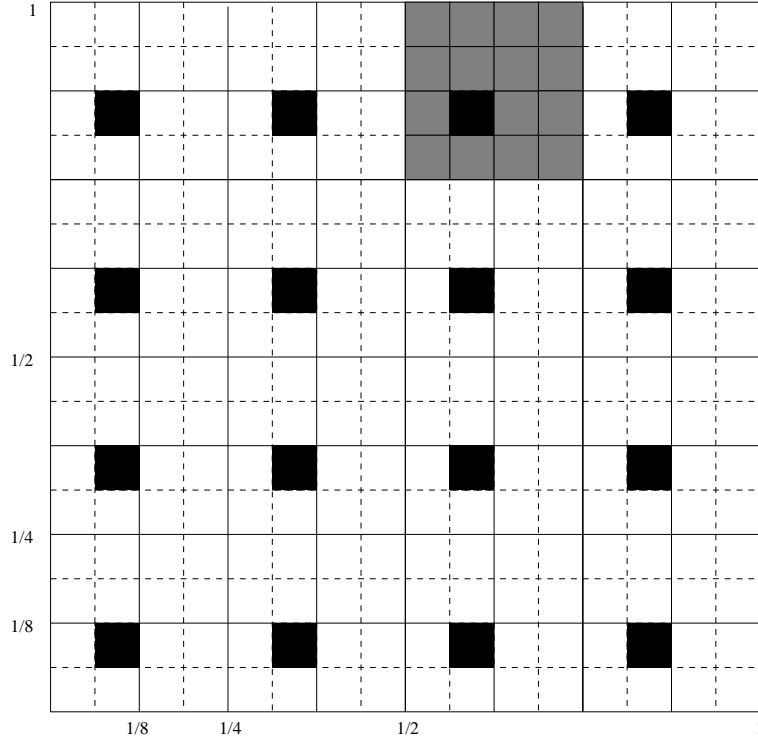


FIG. 1: A schematic illustration of the projectors $P_{\mathbf{y}}^{(l,r)}$ and $P_{\mathbf{y}^1, \mathbf{y}^2}^{(l, m_l, m_r, r)}$. **(a)** Let $n-l = 2$, $N-l-r = 4$, and $\mathbf{y} = y_1 \dots y_4 = 1110$. The projector $P_{\mathbf{y}=1110}^{(l,r)}$ is then in approximate correspondence with the phase space region shaded in grey. **(b)** Let $n-l = 4$, $m_l = 2$, $m_r = 2$, $\mathbf{y}^1 = 10$ and $\mathbf{y}^2 = 01$. The projector $P_{\mathbf{y}^1=10, \mathbf{y}^2=01}^{(l,2,2,r)}$ is then in approximate correspondence with the disconnected phase space region given by the 16 black cells.

where the empty boxes indicate the bits which are coarse-grained over. We can write the projectors of the second type as sums over projectors of the first type:

$$P_{\mathbf{y}^1, \mathbf{y}^2}^{(l, m_l, m_r, r)} = \sum_{\boldsymbol{\xi} \in \{0,1\}^{m_l + m_r}} P_{\mathbf{y}^1 \boldsymbol{\xi} \mathbf{y}^2}^{(l,r)}, \quad (3.7)$$

where $\mathbf{y}^1 \boldsymbol{\xi} \mathbf{y}^2$ means the concatenation of the three strings \mathbf{y}^1 , $\boldsymbol{\xi}$ and \mathbf{y}^2 . Remember that in the definition of the projectors $P_{\mathbf{y}^1, \mathbf{y}^2}^{(l, m_l, m_r, r)}$ we assume that $l + |\mathbf{y}^1| \leq n$ and $r + |\mathbf{y}^2| \leq N - n$.

The projectors (3.5) and (3.6) are special cases of the family of all projection operators, which define the scales at which information is lost in the symbolic representation. In general such projectors exhibit structure on many different scales, and the most general projector

of this type would be of the form

$$P_{\mathbf{y}^1, \mathbf{y}^2, \dots, \mathbf{y}^\lambda}^{(l, m_1, m_2, \dots, m_{\lambda-1}, r)} = \left(\underbrace{\square \dots \square}_l \mathbf{y}^1 \underbrace{\square \dots \square}_{m_1} \mathbf{y}^2 \underbrace{\square \dots \square}_{m_2} \dots \mathbf{y}^{\lambda-1} \underbrace{\square \dots \square}_{m_{\lambda-1}} \mathbf{y}^\lambda \underbrace{\square \dots \square}_r \right). \quad (3.8)$$

The projector (3.8) defines a coarse-graining in which information is lost on several different scales. We will call this a *multi-scale coarse-graining* or *hierarchical coarse-graining*. Accordingly, the special cases (3.5) and (3.6) will be called 1-scale and 2-scale coarse-graining, respectively. The 2-scale coarse-graining (3.6) we introduced above is a special 2-scale coarse-graining, as we assumed that the coarse-grained *island* of size $m_l + m_r$ between the specified strings \mathbf{y}^1 and \mathbf{y}^2 lies around the dot separating the momentum and position bits in the symbolic representation. The first step towards a generalisation is to combine the two parameters m_l and m_r (i.e. the number of most significant momentum and position bits that are coarse-grained over in the symbolic representation) to a single parameter $m = m_l + m_r$ and allow the corresponding coarse-grained island of size m between the specified strings \mathbf{y}^1 and \mathbf{y}^2 to lie anywhere, not necessarily at the most significant region around the dot. The next step is to introduce several coarse-grained islands of this kind, on several scales. An event will then be specified by bit strings $\mathbf{y}^1, \mathbf{y}^2, \dots, \mathbf{y}^\lambda$ of length $|\mathbf{y}^i| = s_i$ at a time, separated by $(\lambda - 1)$ coarse-grained islands of size m_i each, where $\lambda > 1$, as in Eq. (3.8).

More precisely, the most general family of coarse-grained descriptions is represented by sets of projection operators defined as follows:

$$\begin{aligned} P_{\mathbf{y}^1, \mathbf{y}^2, \dots, \mathbf{y}^\lambda}^{(l, m_1, m_2, \dots, m_{\lambda-1}, r)} &\equiv \sum_{\mathbf{a} \in \{0,1\}^l} \sum_{\mathbf{b} \in \{0,1\}^r} \sum_{\xi^1 \in \{0,1\}^{m_1}} \dots \sum_{\xi^{\lambda-1} \in \{0,1\}^{m_{\lambda-1}}} \\ &|\mathbf{a} \mathbf{y}^1 \xi^1 \mathbf{y}^2 \xi^2 \dots \xi^{\lambda-1} \mathbf{y}^\lambda \mathbf{b}\rangle_n \langle \mathbf{a} \mathbf{y}^1 \xi^1 \mathbf{y}^2 \xi^2 \dots \xi^{\lambda-1} \mathbf{y}^\lambda \mathbf{b}| \\ &= \sum_{\xi^1 \in \{0,1\}^{m_1}} \dots \sum_{\xi^{\lambda-1} \in \{0,1\}^{m_{\lambda-1}}} P_{\mathbf{y}^1 \xi^1 \mathbf{y}^2 \xi^2 \dots \mathbf{y}^{\lambda-1} \xi^{\lambda-1} \mathbf{y}^\lambda}^{(l, r)}, \end{aligned} \quad (3.9)$$

where $\mathbf{y}^1 \xi^1 \mathbf{y}^2 \xi^2 \dots \mathbf{y}^{\lambda-1} \xi^{\lambda-1} \mathbf{y}^\lambda$ means the concatenation of the particular strings $\mathbf{y}^1, \xi^1, \mathbf{y}^2, \dots, \xi^{\lambda-1}, \mathbf{y}^\lambda$. We still assume $l < n$ and $r < N - n$. Eq. (3.8) is a diagram notation of Eq. (3.9). It is easily seen that for fixed $m_1, \dots, m_{\lambda-1}$ the set $\{P_{\mathbf{y}^1, \mathbf{y}^2, \dots, \mathbf{y}^\lambda}^{(l, m_1, m_2, \dots, m_{\lambda-1}, r)}\}$ forms a projective partition of the Hilbert space, as

$$\begin{aligned} P_{\mathbf{y}^1, \mathbf{y}^2, \dots, \mathbf{y}^\lambda}^{(l, m_1, m_2, \dots, m_{\lambda-1}, r)} P_{\mathbf{y}'^1, \mathbf{y}'^2, \dots, \mathbf{y}'^\lambda}^{(l, m_1, m_2, \dots, m_{\lambda-1}, r)} &= \delta_{\mathbf{y}^1, \mathbf{y}'^1} \delta_{\mathbf{y}^2, \mathbf{y}'^2} \times \dots \times \delta_{\mathbf{y}^\lambda, \mathbf{y}'^\lambda} P_{\mathbf{y}^1, \mathbf{y}^2, \dots, \mathbf{y}^\lambda}^{(l, m_1, m_2, \dots, m_{\lambda-1}, r)} \\ \text{and } \sum_{\mathbf{y}^1, \mathbf{y}^2, \dots, \mathbf{y}^\lambda} P_{\mathbf{y}^1, \mathbf{y}^2, \dots, \mathbf{y}^\lambda}^{(l, m_1, m_2, \dots, m_{\lambda-1}, r)} &= \mathbf{1}. \end{aligned} \quad (3.10)$$

2. Coarse-grained histories

In order to investigate coarse-grained evolution we now construct coarse-grained histories. By considering different types of histories constructed from different types of coarse-grained projective partitions we obtain different coarse-grained effective evolutions. Our investigation of the coarse-grained evolution of the quantum baker's map starts with the special cases of 1-scale and 2-scale coarse-grainings as defined in Eqs. (3.5) and (3.6). We first compare the different members of the family

$$\left\{ \left\{ P_{\mathbf{y}^1, \mathbf{y}^2}^{(l, m_l, m_r, r)} : \mathbf{y}^1 \in \{0, 1\}^{s_1}, \mathbf{y}^2 \in \{0, 1\}^{s_2} \right\} : l, r, m_l, m_r, s_1, s_2 \in \{0, 1, 2, \dots\} \right. \\ \left. \text{such that } l + s_1 \leq n, r + s_2 \leq N - n \text{ and } l + r + s_1 + s_2 + m_l + m_r = N \right\} \quad (3.11)$$

of coarse-grained descriptions, parameterised by l, r, s_1, s_2, m_l and m_r , with respect to predictability of the evolution. Our results will concern only such members of this family for which s_1 and s_2 are significantly greater than 1, and $s_1 \geq m_l + m_r$. Furthermore, in order to obtain the classical limit of the quantum baker's map, we will be considering only members with very large value for the parameter l , as $\hbar \rightarrow 0$ will correspond to $l \rightarrow \infty$. Finally, the results will show that only $m = m_l + m_r$ matters, and the specification “ m_l most significant momentum bits and m_r most significant position bits are coarse-grained over” therefore be unnecessary. Note that the local 1-scale coarse-graining (3.1) is included in this family as the special case $m_l + m_r = 0$.

The histories corresponding to 1-scale and 2-scale coarse-graining (3.5) and (3.6) will be labelled by finite sequences of strings in the first case and pairs of finite sequences of strings in the second case, respectively:

$$h_{\vec{\mathbf{y}}} \equiv \left(P_{\mathbf{y}^1}^{(l, r)}, P_{\mathbf{y}^2}^{(l, r)}, \dots, P_{\mathbf{y}^k}^{(l, r)} \right) \quad , \quad (3.12)$$

where $\vec{\mathbf{y}} = (\mathbf{y}^1, \dots, \mathbf{y}^k)$ is a sequence of strings $\mathbf{y}^j \in \{0, 1\}^{N-l-r}$, $j = 1, \dots, k$;

$$h_{\vec{\mathbf{y}}^1, \vec{\mathbf{y}}^2} \equiv \left(P_{\mathbf{y}^{1,1}, \mathbf{y}^{1,2}}^{(l, m_l, m_r, r)}, P_{\mathbf{y}^{2,1}, \mathbf{y}^{2,2}}^{(l, m_l, m_r, r)}, \dots, P_{\mathbf{y}^{k,1}, \mathbf{y}^{k,2}}^{(l, m_l, m_r, r)} \right) \quad , \quad (3.13)$$

where $(\vec{\mathbf{y}}^1, \vec{\mathbf{y}}^2) = ((\mathbf{y}^{1,1}, \dots, \mathbf{y}^{k,1}), (\mathbf{y}^{1,2}, \dots, \mathbf{y}^{k,2}))$ is a pair of finite sequences of strings $\mathbf{y}^{j,i} \in \{0, 1\}^{s_i}$, $j = 1, \dots, k$, $i = 1, 2$, labelling the history.

To examine decoherence of this set of histories and calculate its probability distribution we will evaluate the decoherence functional

$$\mathcal{D}_{B, \rho_0}[h_{\vec{y}}, h_{\vec{z}}] = \text{Tr} [P_{\mathbf{y}^k}^{(l,r)} B P_{\mathbf{y}^{k-1}}^{(l,r)} B \cdots P_{\mathbf{y}^1}^{(l,r)} B \rho_0 B^\dagger P_{\mathbf{z}^1}^{(l,r)} \cdots B^\dagger P_{\mathbf{z}^{k-1}}^{(l,r)} B^\dagger P_{\mathbf{z}^k}^{(l,r)}], \quad (3.14)$$

and

$$\begin{aligned} \mathcal{D}_{B, \rho_0}[h_{\vec{y}^1, \vec{y}^2}, h_{\vec{z}^1, \vec{z}^2}] &\equiv \\ &= \text{Tr} [P_{\mathbf{y}^{k,1}, \mathbf{y}^{k,2}}^{(l,m_l,m_r,r)} B P_{\mathbf{y}^{k-1,1}, \mathbf{y}^{k-1,2}}^{(l,m_l,m_r,r)} B \cdots P_{\mathbf{y}^{1,1}, \mathbf{y}^{1,2}}^{(l,m_l,m_r,r)} B \rho_0 B^\dagger P_{\mathbf{z}^{1,1}, \mathbf{z}^{1,2}}^{(l,m_l,m_r,r)} B^\dagger \cdots B^\dagger P_{\mathbf{z}^{k,1}, \mathbf{z}^{k,2}}^{(l,m_l,m_r,r)}], \end{aligned} \quad (3.15)$$

respectively.

Whether the decoherence functional is diagonal or not depends on the initial state ρ_0 . In order to check decoherence of a given set of histories and assign probabilities to them we therefore need to specify the initial state from which the histories start. Here we choose a certain class of states as the initial states for the histories, namely the discrete set of states that are induced via normalisation by the set of projectors defining the histories. We therefore assume the initial state ρ_0 to be of the same form as the events in the histories, i.e. to be proportional to one of the projection operators of the set $\{P_{\mathbf{y}}^{(l,r)}\}$ or $\{P_{\mathbf{y}^1, \mathbf{y}^2}^{(l,m_l,m_r,r)}\}$, respectively:

$$\rho_0 = \rho_{\mathbf{x}}^{(l,r)} \equiv 2^{-(l+r)} P_{\mathbf{x}}^{(l,r)} \equiv 2^{-(l+r)} (\underbrace{\square \square \dots \square}_l \mathbf{x} \underbrace{\square \square \dots \square}_r), \quad (3.16)$$

or

$$\begin{aligned} \rho_0 &= \rho_{\mathbf{x}^1, \mathbf{x}^2}^{(l,m_l,m_r,r)} \equiv 2^{-(l+m_l+m_r+r)} P_{\mathbf{x}^1, \mathbf{x}^2}^{(l,m_l,m_r,r)} \\ &\equiv 2^{-(l+m_l+m_r+r)} (\underbrace{\square \square \dots \square}_l \mathbf{x}^1 \underbrace{\square \square \dots \square}_{m_l} \cdot \underbrace{\square \square \dots \square}_{m_r} \mathbf{x}^2 \underbrace{\square \square \dots \square}_r). \end{aligned} \quad (3.17)$$

The normalisation factor $2^{-(l+r)}$ or $2^{-(l+m_l+m_r+r)}$, respectively, ensures that ρ_0 is a density operator, i.e. $\text{Tr}[\rho_0] = 1$. All calculations in Sec. III C will be based on this choice for the initial states, which we regard as the most natural choice within our framework of sets of histories constructed from a given, fixed projective partition.

We now generalise the family of sets of coarse-grained histories from the 1-scale and 2-scale coarse-grained descriptions considered above to the general case of multi-scale (or

hierarchical) coarse-grainings. The corresponding projective partitions have already been introduced in Eqs. (3.8) and (3.9). The generalised family of coarse-grained descriptions is therefore given by the set:

$$\left\{ \left\{ P_{\mathbf{y}^1, \mathbf{y}^2, \dots, \mathbf{y}^\lambda}^{(l, m_1, m_2, \dots, m_{\lambda-1}, r)} \right\}_{\mathbf{y}^j \in \{0,1\}^{s_j}} : l, r, m_j, s_j \in \{0, 1, 2, \dots\} \quad , \quad \lambda \in \{1, 2, 3, \dots\} \right. \\ \left. \text{such that} \quad l + r + \sum_{j=1}^{\lambda-1} m_j + \sum_{j=1}^{\lambda} s_j = N \right\}. \quad (3.18)$$

The members of this family are represented by coarse-grained projective partitions displaying coarseness on several different scales in the symbolic representation. The family is parameterised by $l, r, m_1, \dots, m_{\lambda-1}, s_1, \dots, s_\lambda$ and λ with the constraint $l + r + \sum_{j=1}^{\lambda-1} m_j + \sum_{j=1}^{\lambda} s_j = N$. Again, our results will involve only such members of this family, for which s_1, \dots, s_λ have values significantly greater than 1, and the value of l is very large (classical limit).

Our generalised type of histories is labelled by (finite) sequences of finite sequences of binary strings:

$$\left\{ h_{\vec{\mathbf{y}}^1, \vec{\mathbf{y}}^2, \dots, \vec{\mathbf{y}}^\lambda} : \vec{\mathbf{y}}^i = (\mathbf{y}^{1,i}, \dots, \mathbf{y}^{k,i}) \quad \text{with} \quad \mathbf{y}^{j,i} \in \{0, 1\}^{s_i} \quad , \quad j = 1, \dots, k \quad , \quad i = 1, \dots, \lambda \right\}. \quad (3.19)$$

They are explicitly defined by time-ordered sequences of (3.9)-type projection operators:

$$h_{\vec{\mathbf{y}}^1, \vec{\mathbf{y}}^2, \dots, \vec{\mathbf{y}}^\lambda} \equiv \left(P_{\mathbf{y}^{1,1}, \mathbf{y}^{1,2}, \dots, \mathbf{y}^{1,\lambda}}^{(l, m_1, m_2, \dots, m_{\lambda-1}, r)} \quad , \quad P_{\mathbf{y}^{2,1}, \mathbf{y}^{2,2}, \dots, \mathbf{y}^{2,\lambda}}^{(l, m_1, m_2, \dots, m_{\lambda-1}, r)} \quad , \dots \quad , \quad P_{\mathbf{y}^{k,1}, \mathbf{y}^{k,2}, \dots, \mathbf{y}^{k,\lambda}}^{(l, m_1, m_2, \dots, m_{\lambda-1}, r)} \right) \quad . \quad (3.20)$$

To examine decoherence of the set of histories (3.19) and calculate its probability distribution we will evaluate the decoherence functional

$$\mathcal{D}_{B, \rho_0} [h_{\vec{\mathbf{y}}^1, \vec{\mathbf{y}}^2, \dots, \vec{\mathbf{y}}^\lambda}, h_{\vec{\mathbf{z}}^1, \vec{\mathbf{z}}^2, \dots, \vec{\mathbf{z}}^\lambda}] \equiv \\ = \text{Tr} \left[P_{\mathbf{y}^{k,1}, \mathbf{y}^{k,2}, \dots, \mathbf{y}^{k,\lambda}}^{(l, m_1, m_2, \dots, m_{\lambda-1}, r)} B P_{\mathbf{y}^{k-1,1}, \mathbf{y}^{k-1,2}, \dots, \mathbf{y}^{k-1,\lambda}}^{(l, m_1, m_2, \dots, m_{\lambda-1}, r)} B \dots P_{\mathbf{y}^{1,1}, \mathbf{y}^{1,2}, \dots, \mathbf{y}^{1,\lambda}}^{(l, m_1, m_2, \dots, m_{\lambda-1}, r)} B \rho_0 B^\dagger \times \right. \\ \left. \times P_{\mathbf{z}^{1,1}, \mathbf{z}^{1,2}, \dots, \mathbf{z}^{1,\lambda}}^{(l, m_1, m_2, \dots, m_{\lambda-1}, r)} B^\dagger \dots P_{\mathbf{z}^{k-1,1}, \mathbf{z}^{k-1,2}, \dots, \mathbf{z}^{k-1,\lambda}}^{(l, m_1, m_2, \dots, m_{\lambda-1}, r)} B^\dagger P_{\mathbf{z}^{k,1}, \mathbf{z}^{k,2}, \dots, \mathbf{z}^{k,\lambda}}^{(l, m_1, m_2, \dots, m_{\lambda-1}, r)} \right], \quad (3.21)$$

Again we will choose the initial state to be proportional to one of the projection operators defining our coarse-grained description, i.e. to one of the (3.9)-type projectors:

$$\rho_0 = \rho_{\mathbf{x}^1, \mathbf{x}^2, \dots, \mathbf{x}^\lambda}^{(l, m_1, m_2, \dots, m_{\lambda-1}, r)} \equiv 2^{-(l+r+m_1+m_2+\dots+m_{\lambda-1})} P_{\mathbf{x}^1, \mathbf{x}^2, \dots, \mathbf{x}^\lambda}^{(l, m_1, m_2, \dots, m_{\lambda-1}, r)}, \quad (3.22)$$

with the normalisation factor ensuring $\text{Tr} [\rho_0] = 1$.

B. Main results

To characterise and quantify predictability, we use the rate of the entropy production. The greater the rate of the entropy production, the more unpredictable is the evolution. We begin by stating the results for the family (3.11) of 1-scale and 2-scale coarse-grainings. First of all we find that in the asymptotic limit $l \rightarrow \infty$ all the corresponding members of this family (i.e., all members with very large parameter value l), provided that $m_l + m_r$ is finite, lead to decoherent sets of histories, which is the prerequisite for classicality. For finite, but very large l the decoherence functional is approximately diagonal, which means approximate decoherence of histories. For very large l , the diagonal elements of the decoherence functional, $\mathcal{D}_{B, \rho_0}[h_{\vec{y}^1}, \vec{y}^2, h_{\vec{y}^1}, \vec{y}^2]$, may therefore be interpreted as probabilities of the corresponding histories. Furthermore we find that for very large l , for all members of the corresponding subset within this family, for which s_1 and s_2 are significantly greater than 1, the probabilities of the individual alternative histories of a set are peaked at histories which display regularities according to the *classical shift property*.

We have compared the rates of entropy increase of the different sets within the family (3.11) of coarse-grainings. The result for the local coarse-graining (3.1), i.e. for the case $m_l + m_r = 0$, was obtained in an earlier work of two of us [19]. In [19] it was shown that in this case the coarse-grained quantum baker's map exhibits a linear entropy increase at an asymptotic rate given by the Kolmogorov-Sinai entropy [13] of the classical chaotic baker's map, namely 1 bit per iteration step:

$$H[\{h_{\vec{y}}\}] = k + O\left(\frac{(l+r-k)\log_2(l+r-k)}{2^{l-2(k^2+k)}}\right), \quad (3.23)$$

where the set $\{h_{\vec{y}}\}$ consists of histories of length k .

For nonlocal coarse-grainings $m_l + m_r \neq 0$, the derivation in the next section give these results:

- Entropy after k iteration steps in case $k \leq m_l + m_r$:

$$H[\{h_{\vec{y}^1}, \vec{y}^2\}] = 2k + O\left(\frac{(l+r-k)\log_2(l+r-k)}{2^{l-2(k^2+(1+m_l+m_r)k)}}\right) \quad (3.24)$$

- Entropy after k iteration steps in case $k \geq m_l + m_r$:

$$H[\{h_{\vec{y}^1}, \vec{y}^2\}] = k + (m_l + m_r) + O\left(\frac{(l+r-k)\log_2(l+r-k)}{2^{l-2(k^2+(1+m_l+m_r)k)}}\right). \quad (3.25)$$

The entropy increase is 2 bits per iteration step as long as the number of iterations k of the quantum baker's map is smaller than $m = m_l + m_r$. As soon as the number of iterations exceeds the parameter m , the rate of entropy increase drops to 1 bit per iteration step. Both short-term and long-term rates of entropy increase are thus independent of the non-locality parameter m . The parameter m determines the duration of the short-term regime for which the entropy increases at a rate of 2 bits per iterations.

Higher rates of entropy increase become possible for hierarchical coarse-grainings, i.e. coarse-grained histories with coarse-graining on several different scales of the phase space. As before we find approximate decoherence for such sets of histories and a probability distribution which is peaked at histories displaying regularities according to the classical shift property. The following results are valid for large l (classical limit) and values for s_j ($j = 1, 2, \dots, \lambda$) that are significantly greater than 1.

- Entropy after k iteration steps in the case $k < \min\{m_1, m_2, \dots, m_{\lambda-1}\}$:

$$H[\{h_{\bar{y}^1, \bar{y}^2, \dots, \bar{y}^\lambda}\}] = \lambda \cdot k + \mathcal{O}\left(\frac{(l+r-k) \log_2(l+r-k)}{2^{l-2(k^2+(1+m_1+m_2+\dots+m_{\lambda-1})k)}}\right) \quad (3.26)$$

- Entropy after k iteration steps in the case $k > \max\{m_1, m_2, \dots, m_{\lambda-1}\}$:

$$H[\{h_{\bar{y}^1, \bar{y}^2, \dots, \bar{y}^\lambda}\}] = k + \sum_{i=1}^{\lambda-1} m_i + \mathcal{O}\left(\frac{(l+r-k) \log_2(l+r-k)}{2^{l-2(k^2+(1+m_1+m_2+\dots+m_{\lambda-1})k)}}\right). \quad (3.27)$$

We see that in the long-term regime, $k > \max\{m_1, m_2, \dots, m_{\lambda-1}\}$, the rate of entropy increase is again 1 bit per iteration, independently of the character of the coarse-graining. In the short-term regime, $k < \min\{m_1, m_2, \dots, m_{\lambda-1}\}$, however, the rate of entropy increase is λ bits per iteration. The short-term regime is thus characterised by λ , the number of coarse-graining scales. The parameters $m_1, \dots, m_{\lambda-1}$ determine the duration of the short-term regime. Classical predictability decreases with increasing number of coarse-graining scales.

Finally, we note how the above results for the entropy production in the various coarse-grained descriptions can be understood using the shift property of the coarse-grained evolution of the quantum baker's map, which is explained and illustrated in detail in the next section. For this we make use of our diagram notation (3.8). The shift property implies that the only histories with significant probabilities are those that satisfy the shift condition, i.e., the projectors of the histories have to be related to the initial state via a shift.

For instance, if $\rho_0 \propto P_{\mathbf{x}^1, \mathbf{x}^2, \dots, \mathbf{x}^\lambda}^{(l, m_1, m_2, \dots, m_{\lambda-1}, r)}$, then only such histories can arise with significant probabilities whose first event, represented by the projector $P_{\mathbf{y}^{1,1}, \mathbf{y}^{1,2}, \dots, \mathbf{y}^{1,\lambda}}^{(l, m_1, m_2, \dots, m_{\lambda-1}, r)}$, satisfies the shift constraint. Unless $\mathbf{y}_{1:(s_1-1)}^{1,1} = \mathbf{x}_{2:s_1}^1$ and $\mathbf{y}_{1:(s_2-1)}^{1,2} = \mathbf{x}_{2:s_2}^2$ and \dots and $\mathbf{y}_{1:(s_\lambda-1)}^{1,\lambda} = \mathbf{x}_{2:s_\lambda}^\lambda$ is satisfied by the first event the whole history will have a vanishing probability. On the other hand the last bits $y_{s_1}^{1,1}, y_{s_2}^{1,2}, \dots, y_{s_\lambda}^{1,\lambda}$ of the strings $\mathbf{y}^{1,1}, \mathbf{y}^{1,2}, \dots, \mathbf{y}^{1,\lambda}$, which denote the first event of the history, remain undetermined, because the unspecified bits of the empty boxes in (3.8), which are coarse-grained over, are shifted onto them. The bits $y_{s_1}^{1,1}, y_{s_2}^{1,2}, \dots, y_{s_\lambda}^{1,\lambda}$ may therefore be chosen arbitrarily, corresponding to a branching into 2^λ possible histories with non-vanishing probabilities. This branching into 2^λ alternatives repeats with each iteration step of the evolution, as long as $k < \min\{m_1, m_2, \dots, m_{\lambda-1}\}$, leading to an entropy production of λ bits per iteration step. As soon as the number of iterations k starts to exceed, step by step, the values of $m_1, m_2, \dots, m_{\lambda-1}$, the rate of entropy production goes down, step by step, from the value λ to the value 1 in the long-term regime. Consider, for instance, the case in which $k > m_{\lambda-1}$. Only in the first $m_{\lambda-1}$ iteration steps coarse-grained bits (the empty boxes of our diagram notation) are shifted onto the last bits of the strings $\mathbf{y}^{j,\lambda-1}$, thereby making them arbitrarily chose-able for the history, causing a branching into two alternatives, and increasing the entropy by 1 bit. In the subsequent $k - m_{\lambda-1}$ iterations the string \mathbf{x}^λ of the initial condition enters the scale of the $\mathbf{y}^{j,\lambda-1}$ -strings, with the consequence that the last bits of the strings $\mathbf{y}^{m_{\lambda-1}+1,\lambda-1}, \dots, \mathbf{y}^{k,\lambda-1}$ become determined by the initial condition, meaning no branching and therefore no entropy increase.

C. Derivation and illustration of the results

1. 1-scale and 2-scale coarse-grainings

The decoherence functional for the locally coarse-grained histories (3.14) was calculated in an earlier work of two of the authors [19]. We briefly review the corresponding result, which is:

$$\mathcal{D}_{B, \rho_{\mathbf{x}}^{(l,r)}}[h_{\bar{\mathbf{y}}}, h_{\bar{\mathbf{z}}}] = 2^{-k} \underbrace{\left(\prod_{j=1}^k \delta_{\mathbf{y}^j}^{z^j} \right)}_{\text{diagonal}} \cdot \underbrace{\left(\delta_{\mathbf{y}_{1:\gamma-1}^1}^{\mathbf{x}_{2:\gamma}} \prod_{j=1}^{k-1} \delta_{\mathbf{y}_{1:\gamma-1}^{j+1}}^{\mathbf{y}_{1:\gamma}^j} \right)}_{\text{step-by-step shift}} \cdot \underbrace{\left(\delta_{\mathbf{y}_{1:\gamma-k}^k}^{\mathbf{x}_{k+1:\gamma}} \right)}_{k\text{th shift}} + O\left(\frac{l+r-k}{2^{l-2(k^2+k)}}\right), \quad (3.28)$$

where $\gamma \equiv |\mathbf{x}| = |\mathbf{y}^j| = |\mathbf{z}^j| = N - (l + r)$. The expression in the first parentheses is zero for all off-diagonal elements of the decoherence functional. In the limit of very large l all off-diagonal elements of the decoherence functional vanish, the decoherence condition being therefore established. The diagonal elements of the decoherence functional can therefore be interpreted as probabilities of the corresponding histories (see Ref. [6] for a discussion of approximate decoherence). Asymptotically, only 2^k diagonal elements survive. Moreover, the error terms are exponentially small. We therefore get 2^k histories with asymptotically equal probabilities. The number of such histories doubles after each iteration step resulting in a loss of information at the rate of 1 bit per step. This information loss is quantified by the entropy increase of the set of histories. Since in the limit of large l the set of histories $\{h_{\vec{y}}\}$ is decoherent, the individual alternative histories may be assigned probabilities, which are then given by $p[h_{\vec{y}}] = \mathcal{D}_{B, \rho_{\mathbf{x}}^{(l,r)}}[h_{\vec{y}}, h_{\vec{y}}]$. Having found the probability distribution we may also define the entropy of the set of all possible alternative histories:

$$\begin{aligned} H[\{h_{\vec{y}}\}] &\equiv - \sum_{\vec{y}} p[h_{\vec{y}}] \log_2 p[h_{\vec{y}}] \\ &\equiv - \sum_{\vec{y}} \mathcal{D}_{B, \rho_{\mathbf{x}}^{(l,r)}}[h_{\vec{y}}, h_{\vec{y}}] \log_2 \left(\mathcal{D}_{B, \rho_{\mathbf{x}}^{(l,r)}}[h_{\vec{y}}, h_{\vec{y}}] \right). \end{aligned} \quad (3.29)$$

With (3.28) we obtain:

$$H[\{h_{\vec{y}}\}] = k + O\left(\frac{(l + r - k) \log_2(l + r - k)}{2^{l-2(k^2+k)}}\right). \quad (3.30)$$

In the limit of large l , for any fixed number of iterations, k , the entropy of the coarse-grained quantum baker's map approaches the value of k bits, i.e., 1 bit per iteration.

What kind of histories arise with significant probabilities? This is determined by the expressions within the second and third parentheses of the result (3.28). Accordingly only histories that satisfy a *step-by-step shift condition* arise with significant probabilities. This can be illustrated using the diagram notation introduced above:

$$\begin{array}{c} \underbrace{\square \square \dots \square}_l \quad \mathbf{x}_1 \mathbf{x}_2 \dots \mathbf{x}_{\gamma-2} \mathbf{x}_{\gamma-1} \mathbf{x}_\gamma \quad \underbrace{\square \square \dots \square}_r, \\ \swarrow \\ \underbrace{\square \square \dots \square}_l \quad \overline{\mathbf{y}_1^1 \mathbf{y}_2^1 \dots \mathbf{y}_{\gamma-2}^1 \mathbf{y}_{\gamma-1}^1} \mathbf{y}_\gamma^1 \quad \underbrace{\square \square \dots \square}_r, \\ \swarrow \\ \underbrace{\square \square \dots \square}_l \quad \overline{\mathbf{y}_1^2 \mathbf{y}_2^2 \dots \mathbf{y}_{\gamma-2}^2 \mathbf{y}_{\gamma-1}^2} \mathbf{y}_\gamma^2 \quad \underbrace{\square \square \dots \square}_r, \end{array}$$

$$\begin{array}{c}
\swarrow \\
\dots \\
\swarrow \\
\underbrace{\square \square \dots \square}_l \overline{\mathbf{y}_1^k \dots \mathbf{y}_{\gamma-k}^k \mathbf{y}_{\gamma-k+1}^k \dots \mathbf{y}_\gamma^k} \underbrace{\square \square \dots \square}_r .
\end{array} \tag{3.31}$$

The first line of this diagram represents the initial condition $\rho_{\mathbf{x}}^{(l,r)}$. The subsequent lines correspond to the projectors $P_{\mathbf{y}^1}^{(l,r)}, \dots, P_{\mathbf{y}^k}^{(l,r)}$ constituting the history $h_{\vec{\mathbf{y}}}$. The step-by-step shift condition is depicted by arrows and lines. Underlined substrings are shifted onto those overlined substrings which are indicated by arrows. In order to fulfil the step-by-step shift condition all underlined and overlined substrings that are connected by an arrow have to be equal. In this way it becomes clear which bits of the symbolic specification of a history are completely determined by the initial condition. These bits are in bold face. The other bits may be chosen arbitrarily. For instance, in the first iteration step the initial condition substring $\mathbf{x}_{2:\gamma} \equiv x_2 \dots x_\gamma$ is shifted onto the substring $\mathbf{y}_{1:\gamma-1}^1 \equiv y_1^1 \dots y_{\gamma-1}^1$. The first $\gamma - 1$ bits of the string \mathbf{y}^1 of the first event in the history $h_{\vec{\mathbf{y}}}$ are therefore determined by the initial condition. Unless $\mathbf{y}_{1:\gamma-1}^1 = \mathbf{x}_{2:\gamma}$ is satisfied by the first event, the whole history will have a vanishing probability. On the other hand the last bit y_γ^1 of the string \mathbf{y}^1 , which denotes the first event of the history, remains undetermined, because the unspecified bit of the empty box is shifted onto it, which is coarse-grained (i.e. summed) over. The bit y_γ^1 may therefore be chosen arbitrarily, corresponding to a branching into two possible histories with non-vanishing probabilities and therefore an entropy increase of 1 bit. This procedure repeats with each iteration step of the evolution. For the entire history, therefore, there are only k independent bits which can be chosen arbitrarily, given the step-by-step shift constraint.

The calculation of the decoherence functional (3.15) for the non-locally coarse-grained histories can be traced back to using the above result for the local ones. To do so, we may express all the nonlocal projection operators appearing in the decoherence functional as sums over suitable local ones:

$$\rho_{\mathbf{x}^1, \mathbf{x}^2}^{(l, m_l, m_r, r)} = 2^{-(l+m_l+m_r+r)} \sum_{\boldsymbol{\xi} \in \{0,1\}^{m_l+m_r}} P_{\mathbf{x}^1 \boldsymbol{\xi} \mathbf{x}^2}^{(l,r)} , \tag{3.32}$$

$$P_{\mathbf{y}^{j,1}, \mathbf{y}^{j,2}}^{(l, m_l, m_r, r)} = \sum_{\boldsymbol{\eta}^j \in \{0,1\}^{m_l+m_r}} P_{\mathbf{y}^{j,1} \boldsymbol{\eta}^j \mathbf{y}^{j,2}}^{(l,r)} , \quad j = 1, 2, \dots, k , \tag{3.33}$$

$$P_{\mathbf{z}^{j,1}, \mathbf{z}^{j,2}}^{(l, m_l, m_r, r)} = \sum_{\boldsymbol{\zeta}^j \in \{0,1\}^{m_l+m_r}} P_{\mathbf{z}^{j,1} \boldsymbol{\zeta}^j \mathbf{z}^{j,2}}^{(l,r)} , \quad j = 1, 2, \dots, k . \tag{3.34}$$

By inserting these expressions into the decoherence functional (3.15) we arrive at:

$$\begin{aligned}
\mathcal{D}_{B, \rho_0}[h_{\bar{\mathbf{y}}^1}, \bar{\mathbf{y}}^2, h_{\bar{\mathbf{z}}^1}, \bar{\mathbf{z}}^2] &= \\
&= \sum_{\boldsymbol{\eta}^1 \in \{0,1\}^{m_l+m_r}} \cdots \sum_{\boldsymbol{\eta}^k \in \{0,1\}^{m_l+m_r}} \sum_{\boldsymbol{\xi} \in \{0,1\}^{m_l+m_r}} \sum_{\boldsymbol{\zeta}^1 \in \{0,1\}^{m_l+m_r}} \cdots \sum_{\boldsymbol{\zeta}^k \in \{0,1\}^{m_l+m_r}} \\
&2^{-(m_l+m_r)} \text{Tr} \left[P_{\mathbf{y}^{k,1} \boldsymbol{\eta}^k \mathbf{y}^{k,2}}^{(l,r)} B P_{\mathbf{y}^{k-1,1} \boldsymbol{\eta}^{k-1} \mathbf{y}^{k-1,2}}^{(l,r)} B \cdots B P_{\mathbf{y}^{1,1} \boldsymbol{\eta}^1 \mathbf{y}^{1,2}}^{(l,r)} \times \right. \\
&\times \left. B \left(\frac{1}{2^{l+r}} P_{\mathbf{x}^1 \boldsymbol{\xi} \mathbf{x}^2}^{(l,r)} \right) B^\dagger P_{\mathbf{z}^{1,1} \boldsymbol{\zeta}^1 \mathbf{z}^{1,2}}^{(l,r)} B^\dagger \cdots P_{\mathbf{z}^{k-1,1} \boldsymbol{\zeta}^{k-1} \mathbf{z}^{k-1,2}}^{(l,r)} B^\dagger P_{\mathbf{z}^{k,1} \boldsymbol{\zeta}^k \mathbf{z}^{k,2}}^{(l,r)} \right]
\end{aligned} \tag{3.35}$$

Each term of the sum over all possible strings $\boldsymbol{\xi}$, $\{\boldsymbol{\eta}^j\}$ and $\{\boldsymbol{\zeta}^j\}$ is, apart from the factor $2^{-(m_l+m_r)}$, a decoherence functional with respect to histories composed of local projectors. Each such term, therefore, results in an expression of the form (3.28), and we obtain:

$$\begin{aligned}
\mathcal{D}_{B, \rho_0}[h_{\bar{\mathbf{y}}^1}, \bar{\mathbf{y}}^2, h_{\bar{\mathbf{z}}^1}, \bar{\mathbf{z}}^2] &= \\
&= \sum_{\boldsymbol{\eta}^1 \in \{0,1\}^{m_l+m_r}} \cdots \sum_{\boldsymbol{\eta}^k \in \{0,1\}^{m_l+m_r}} \sum_{\boldsymbol{\xi} \in \{0,1\}^{m_l+m_r}} \sum_{\boldsymbol{\zeta}^1 \in \{0,1\}^{m_l+m_r}} \cdots \sum_{\boldsymbol{\zeta}^k \in \{0,1\}^{m_l+m_r}} 2^{-(m_l+m_r)} \times \\
&\times \left\{ \underbrace{2^{-k} \left(\prod_{i=1}^k \delta_{\mathbf{y}^{i,1} \boldsymbol{\eta}^i \mathbf{y}^{i,2}}^{z^{i,1} \boldsymbol{\zeta}^i z^{i,2}} \right)}_{\text{diagonal}} \cdot \underbrace{\left(\delta_{\mathbf{y}^{1,1} \boldsymbol{\eta}^1 \mathbf{y}^{1,2}}^{x_1^1 \boldsymbol{\xi} x_2^1} \prod_{j=1}^{k-1} \delta_{\mathbf{y}^{j+1,1} \boldsymbol{\eta}^{j+1} \mathbf{y}^{j+1,2}}^{y_2^{j,1} \boldsymbol{\eta}^j y_1^{j,2}} \right)}_{\text{step-by-step shift}} \right\} \times \\
&\times \left\{ \underbrace{\left(\delta_{(\mathbf{y}^{k,1} \boldsymbol{\eta}^k \mathbf{y}^{k,2})_{1:\gamma-k}}^{(x^1 \boldsymbol{\xi} x^2)_{k+1:\gamma}} \right)}_{k\text{th shift}} + \mathcal{O}\left(\frac{l+r-k}{2^{l-2(k^2+k)}}\right) \right\} \\
&= \sum_{\boldsymbol{\eta}^1 \in \{0,1\}^{m_l+m_r}} \cdots \sum_{\boldsymbol{\eta}^k \in \{0,1\}^{m_l+m_r}} \sum_{\boldsymbol{\xi} \in \{0,1\}^{m_l+m_r}} \left\{ 2^{-(m_l+m_r)} \cdot 2^{-k} \cdot \underbrace{\left(\prod_{i=1}^k \delta_{\mathbf{y}^{i,1} \boldsymbol{\eta}^i \mathbf{y}^{i,2}}^{z^{i,1} \boldsymbol{\zeta}^i z^{i,2}} \right)}_{\text{diagonal}} \right\} \times \\
&\times \underbrace{\left(\delta_{\mathbf{y}^{1,1}}^{x_2^1 s_1 \boldsymbol{\xi} 1} \delta_{\boldsymbol{\eta}^1}^{x_2^1 (m_l+m_r) \boldsymbol{\xi} 1} \delta_{\mathbf{y}^{1,2}}^{x_2^1 s_2} \prod_{j=1}^{k-1} \delta_{\mathbf{y}^{j+1,1}}^{y_2^{j,1} \boldsymbol{\eta}^j} \delta_{\boldsymbol{\eta}^{j+1}}^{y_2^{j,1} \boldsymbol{\eta}^j} \delta_{\mathbf{y}^{j,2}}^{y_1^{j,2}} \delta_{\mathbf{y}^{1,2}}^{y_1^{j+1,2}} \right)}_{\text{step-by-step shift}} \times \\
&\times \left\{ \underbrace{\left(\delta_{(\mathbf{y}^{k,1} \boldsymbol{\eta}^k \mathbf{y}^{k,2})_{1:\gamma-k}}^{(x^1 \boldsymbol{\xi} x^2)_{k+1:\gamma}} \right)}_{k\text{th shift}} \right\} + \left(2^{m_l+m_r} \right)^{2k} \cdot \mathcal{O}\left(\frac{l+r-k}{2^{l-2(k^2+k)}}\right)
\end{aligned} \tag{3.36}$$

Here γ denotes the length of the strings $\mathbf{y}^{j,1} \boldsymbol{\eta}^j \mathbf{y}^{j,2}$ and $\mathbf{x}^1 \boldsymbol{\xi} \mathbf{x}^2$, respectively, i.e. $\gamma = |\mathbf{x}^1 \boldsymbol{\xi} \mathbf{x}^2| = |\mathbf{y}^{j,1} \boldsymbol{\eta}^j \mathbf{y}^{j,2}| = s_1 + (m_l + m_r) + s_2$.

First of all the sum over all possible $\zeta^j \in \{0, 1\}^{m_l+m_r}$, $j = 1, \dots, k$, collapses due to the term $\prod_{i=1}^k \delta_{\mathbf{y}^{i,1} \boldsymbol{\eta}^i \mathbf{z}^{i,2}}$, apart from contributing a factor $2^{k(m_l+m_r)}$ to the error term. Secondly we note that the step-by-step shift condition causes the whole sum $\sum_{\boldsymbol{\eta}^1} \sum_{\boldsymbol{\eta}^2} \dots \sum_{\boldsymbol{\eta}^k}$ to collapse, apart from contributing a further factor $2^{k(m_l+m_r)}$ to the bound on the error term, which is furthermore enlarged by a factor $2^{(m_l+m_r)}$ stemming from the sum $\sum_{\boldsymbol{\xi}}$. Let us comprehend the collapse of the sums $\sum_{\boldsymbol{\eta}^j}$. For a given fixed string $\boldsymbol{\xi}$ out of the sum $\sum_{\boldsymbol{\xi}}$ all $\boldsymbol{\eta}^1, \boldsymbol{\eta}^2, \dots, \boldsymbol{\eta}^k$ are through the δ 's determined by the string $\boldsymbol{\xi}$ and the given fixed string \mathbf{x}^2 of the initial condition. The first shift leads to a determination of $\boldsymbol{\eta}^1$: according to $\delta_{\boldsymbol{\eta}^1}^{\boldsymbol{\xi}_{2:(m_l+m_r)} \mathbf{x}_1^2}$ the sum over all possible $\boldsymbol{\eta}^1 \in \{0, 1\}^{m_l+m_r}$ collapses and only the string $\boldsymbol{\eta}^1 \stackrel{\perp}{=} \boldsymbol{\xi}_{2:(m_l+m_r)} \mathbf{x}_1^2$ survives. The second shift determines $\boldsymbol{\eta}^2$, since according to $\delta_{\boldsymbol{\eta}^2}^{\boldsymbol{\eta}_{2:(m_l+m_r)}^1 \mathbf{y}_1^{1,2}}$ the sum over all possible $\boldsymbol{\eta}^2 \in \{0, 1\}^{m_l+m_r}$ collapses and only the string $\boldsymbol{\eta}^2 = \boldsymbol{\eta}_{2:(m_l+m_r)}^1 \mathbf{y}_1^{1,2} \equiv \boldsymbol{\xi}_{3:(m_l+m_r)} \mathbf{x}_1^2 \mathbf{x}_2^2$ does lead to a non-vanishing contribution to the decoherence functional. It is easy to see that due to the step-by-step shift condition all the sums $\sum_{\boldsymbol{\eta}^j}$, $j = 1, \dots, k$, collapse and only the strings

$$\boldsymbol{\eta}^j = \boldsymbol{\xi}_{(j+1):(m_l+m_r)} \mathbf{x}_{1:j}^2 \quad (3.37)$$

out of these sums survive leading together to a non-vanishing contribution to the decoherence functional. In fact the step-by-step shift condition can also be expressed in the following way:

$$\prod_{j=1}^k \delta_{(\mathbf{y}^{j,1} \boldsymbol{\eta}^j \mathbf{y}^{j,2})_{1:\gamma-j}}^{(\mathbf{x}^1 \boldsymbol{\xi} \mathbf{x}^2)_{j+1:\gamma}} \quad , \quad (3.38)$$

meaning that only such strings $\boldsymbol{\eta}^j$ out of the corresponding sums $\sum_{\boldsymbol{\eta}^j}$, $j = 1, \dots, k$, lead to a non-vanishing contribution to the decoherence functional which are determined by $\boldsymbol{\xi}$ and \mathbf{x}^2 according to (3.37). Next we note that as a consequence of the step-by-step shift condition also the sum over all possible $\boldsymbol{\xi} \in \{0, 1\}^{m_l+m_r}$ collapses. It collapses only *partially* in case $k < m_l + m_r$ and it collapses *completely* in case $k \geq m_l + m_r$. Let us first consider the case $k < m_l + m_r$. After the first shift the first bit of $\boldsymbol{\xi}$ is determined by the last bit of the string $\mathbf{y}^{1,1}$ of the given history, i.e. $\xi_1 \stackrel{\perp}{=} y_{s_1}^{1,1}$, according to the term $\delta_{\mathbf{y}^{1,1}}^{\mathbf{x}_{2:s_1}^1 \xi_1}$. The second shift leads to $\delta_{\mathbf{y}_{2,1}^{1,1} \boldsymbol{\eta}_1^1}$, so that $\eta_1^1 = y_{s_1}^{2,1}$. But we have $\eta_1^1 = \xi_2$ due to the first shift, so we arrive at a determination of ξ_2 , namely $\xi_2 = y_{s_1}^{2,1}$. In this way the sum over all possible

$\xi \in \{0, 1\}^{m_l+m_r}$ collapses to a sum over all possible $\xi_{(k+1):(m_l+m_r)} \in \{0, 1\}^{m_l+m_r-k}$,

$$\sum_{\xi \in \{0,1\}^{m_l+m_r}} \longrightarrow \sum_{\xi_{(k+1):(m_l+m_r)} \in \{0,1\}^{m_l+m_r-k}}, \quad (3.39)$$

since the first k bits ξ_1, \dots, ξ_k out of the sum \sum_{ξ} have to fulfil the step-by-step shift condition and are therefore determined by $\xi_j = y_{s_1}^{j,1}$. That the first k bits of the string ξ out of the sum \sum_{ξ} are determined by the given history $h_{\bar{y}^1, \bar{y}^2}$ and therefore the sum over the first k bits of $\xi = \xi_1 \xi_2 \dots \xi_{m_l+m_r}$ collapses can also be seen by looking at the k -th shift factor which in fact appears as a redundant factor in the result: according to $\delta_{(\mathbf{y}^{k,1} \boldsymbol{\eta}^k \mathbf{y}^{k,2})_{1:\gamma-k}}^{(\mathbf{x}^1 \boldsymbol{\xi} \mathbf{x}^2)_{k+1:\gamma}}$ only such strings ξ out of the sum \sum_{ξ} lead to a non-vanishing contribution to the decoherence functional for which $\xi_{1:k} = \mathbf{y}_{(s_1-k+1):s_1}^{k,1}$ holds. The remaining $m_l + m_r - k$ bits of $\xi = \xi_1 \xi_2 \dots \xi_{m_l+m_r}$ remain undetermined and are still summed over. There are $2^{m_l+m_r-k}$ possible different substrings $\xi_{k+1:m_l+m_r} \in \{0, 1\}^{m_l+m_r-k}$ in this remaining sum leading to a non-vanishing contribution to the decoherence functional. Since the contributions of all these strings are equal, as can be seen by looking at the result, we may replace the remaining sum over all possible $\xi_{k+1:m_l+m_r}$ by the factor $2^{m_l+m_r-k}$. Furthermore all the δ -terms containing bits of the unspecified strings ξ and $\boldsymbol{\eta}^j$, $j = 1, \dots, k$, which are summed over, may now be replaced by 1 after having been exploited for the determination of that strings ξ and $\boldsymbol{\eta}^j$ out of the sums \sum_{ξ} and $\sum_{\boldsymbol{\eta}^1} \sum_{\boldsymbol{\eta}^2} \dots \sum_{\boldsymbol{\eta}^k}$ which lead to a non-vanishing contribution to the value of the decoherence functional. In case $k < m_l + m_r$ we therefore arrive at the following result:

- Decoherence functional in case $k < m_l + m_r$:

$$\begin{aligned} \mathcal{D}_{B, \rho_0}[h_{\bar{y}^1, \bar{y}^2}, h_{\bar{z}^1, \bar{z}^2}] &= \underbrace{2^{m_l+m_r-k} \cdot 2^{-(m_l+m_r)} \cdot 2^{-k}}_{= 2^{-2k}} \cdot \underbrace{\left(\prod_{i=1}^k \delta_{\mathbf{y}^{i,1}} \delta_{\mathbf{y}^{i,2}} \right)}_{\text{diagonal}} \times \\ &\times \underbrace{\left(\delta_{\mathbf{y}_{1:s_1-1}^{1,1}} \delta_{\mathbf{y}_{1:s_2-1}^{2,2}} \cdot \prod_{j=1}^{k-1} \delta_{\mathbf{y}_{1:s_1-1}^{j,1}} \delta_{\mathbf{y}_{1:s_2-1}^{j,2}} \right)}_{\text{step-by-step shift}} \times \\ &\times \underbrace{\left(\delta_{\mathbf{y}_{1:s_1-k}^{k,1}} \delta_{\mathbf{y}_{1:s_2-k}^{k,2}} \right)}_{k\text{th shift}} + \mathcal{O}\left(\frac{l+r-k}{2^{l-2(k^2+(1+m_l+m_r)k)}}\right). \end{aligned} \quad (3.40)$$

Let us now consider the case $k \geq m_l + m_r$. As already mentioned in this case the whole sum \sum_{ξ} collapses to a single string $\xi \in \{0, 1\}^{m_l+m_r}$ satisfying the step-by-step shift condition. This can be seen, again, by looking at the k -th shift condition given by the factor

$\delta_{(\mathbf{y}^{k,1}\boldsymbol{\eta}^k\mathbf{y}^{k,2})_{1:\gamma-k}}^{(\mathbf{x}^1\xi\mathbf{x}^2)_{k+1:\gamma}}$; according to it each string ξ out of the sum \sum_{ξ} is shifted onto $(m_l + m_r)$ bits of the string $\mathbf{y}^{k,1}$, but since $\mathbf{y}^{k,1}$ is a *fixed* string specifying the last event of the *given* history, only the string $\xi = \mathbf{y}_{(s_1-k+1):(s_1-k+m_l+m_r)}^{k,1}$ out of the sum \sum_{ξ} survives. Of course we presupposed, or had to require, that $s_1 \geq k \geq m_l + m_r$. In case $k \geq m_l + m_r$ we therefore get:

- Decoherence functional in case $k \geq m_l + m_r$:

$$\begin{aligned}
\mathcal{D}_{B,\rho_0}[h_{\bar{\mathbf{y}}^1}, \bar{\mathbf{y}}^2, h_{\bar{\mathbf{z}}^1}, \bar{\mathbf{z}}^2] &= 2^{-(m_l+m_r)} \cdot 2^{-k} \cdot \underbrace{\left(\prod_{i=1}^k \delta_{\mathbf{y}^{i,1}}^{z^{i,1}} \delta_{\mathbf{y}^{i,2}}^{z^{i,2}} \right)}_{\text{diagonal}} \times \\
&\times \underbrace{\left(\delta_{\mathbf{y}_{1:s_1-1}}^{\mathbf{x}_{2:s_1}^1} \delta_{\mathbf{y}_{1:s_2-1}}^{\mathbf{x}_{2:s_2}^2} \cdot \prod_{j=1}^{k-1} \delta_{\mathbf{y}_{1:s_1-1}}^{\mathbf{y}_{2:s_1}^{j,1}} \delta_{\mathbf{y}_{1:s_2-1}}^{\mathbf{y}_{2:s_2}^{j,2}} \right)}_{\text{step-by-step shift}} \times \quad (3.41) \\
&\times \underbrace{\left(\delta_{\mathbf{y}_{1:s_1-k}}^{\mathbf{x}_{k+1:s_1}^1} \delta_{\mathbf{y}_{s_1-k+(m_l+m_r)+1:s_1}}^{\mathbf{x}_{1:k-(m_l+m_r)}^2} \delta_{\mathbf{y}_{1:s_2-k}}^{\mathbf{x}_{k+1:s_2}^2} \right)}_{\text{kth shift}} \\
&+ \mathcal{O}\left(\frac{l+r-k}{2^{l-2(k^2+(1+m_l+m_r)k)}}\right).
\end{aligned}$$

Let us now discuss the results (3.40) and (3.41) for the decoherence functional (3.15). First of all we get approximate decoherence: for very large l the decoherence functional is approximately diagonal. In the asymptotic limit $l \rightarrow \infty$ our set of histories $\{h_{\bar{\mathbf{y}}^1}, \bar{\mathbf{y}}^2\}$ becomes decoherent. The diagonal elements of the functional, $\mathcal{D}_{B,\rho_0}[h_{\bar{\mathbf{y}}^1}, \bar{\mathbf{y}}^2, h_{\bar{\mathbf{y}}^1}, \bar{\mathbf{y}}^2]$, may therefore be interpreted as probabilities of the corresponding histories, i.e. $p(h_{\bar{\mathbf{y}}^1}, \bar{\mathbf{y}}^2,) = \mathcal{D}_{B,\rho_0}[h_{\bar{\mathbf{y}}^1}, \bar{\mathbf{y}}^2, h_{\bar{\mathbf{y}}^1}, \bar{\mathbf{y}}^2]$. Again there is no single dominant history. Several different histories arise with significant probabilities. In case $k < m_l + m_r$ we get 2^{2k} different histories with asymptotically equal probabilities (given by 2^{-2k}). The number of histories with asymptotically nonzero probabilities becomes four times larger after each iteration step of the quantum baker's map resulting in a *loss of information of 2 bits per step*. The entropy increase is therefore *2 bits per iteration step*, which can also be seen by calculating the entropy of the approximately decoherent set of histories $\{h_{\bar{\mathbf{y}}^1}, \bar{\mathbf{y}}^2\}$:

- Entropy after k iteration steps in case $k \leq m_l + m_r$:

$$\begin{aligned}
H[\{h_{\bar{\mathbf{y}}^1, \bar{\mathbf{y}}^2}\}] &= - \sum_{\bar{\mathbf{y}}^1, \bar{\mathbf{y}}^2} p[h_{\bar{\mathbf{y}}^1, \bar{\mathbf{y}}^2}] \log_2 p[h_{\bar{\mathbf{y}}^1, \bar{\mathbf{y}}^2}] \\
&= 2k + \mathcal{O}\left(\frac{(l+r-k) \log_2(l+r-k)}{2^{l-2(k^2+(1+m_l+m_r)k)}}\right). \tag{3.42}
\end{aligned}$$

Again, only such histories are allowed to arise with significant probabilities that satisfy the shift condition: the projectors of the histories have to be related to the initial state via a shift. Let us illustrate this issue once again by means of our diagram notation:

$$\begin{array}{c}
\begin{array}{ccc}
\underbrace{\square \square \dots \square}_l & \mathbf{x}_1^1 \mathbf{x}_2^1 \dots \mathbf{x}_{s_1-2}^1 \mathbf{x}_{s_1-1}^1 \mathbf{x}_{s_1}^1 & \underbrace{\square \square \dots \square}_{m_l+m_r} \\
& \swarrow & \searrow \\
\underbrace{\square \square \dots \square}_l & \overline{\mathbf{y}_1^{1,1} \mathbf{y}_2^{1,1} \dots \mathbf{y}_{s_1-2}^{1,1} \mathbf{y}_{s_1-1}^{1,1} \mathbf{y}_{s_1}^{1,1}} & \underbrace{\square \square \dots \square}_{m_l+m_r} \\
& \swarrow & \searrow \\
\underbrace{\square \square \dots \square}_l & \overline{\mathbf{y}_1^{2,1} \mathbf{y}_2^{2,1} \dots \mathbf{y}_{s_1-2}^{2,1} \mathbf{y}_{s_1-1}^{2,1} \mathbf{y}_{s_1}^{2,1}} & \underbrace{\square \square \dots \square}_{m_l+m_r} \\
& \swarrow & \searrow \\
& \dots & \dots \\
& \swarrow & \searrow \\
\underbrace{\square \square \dots \square}_l & \overline{\mathbf{y}_1^{k,1} \dots \mathbf{y}_{s_1-k}^{k,1} \mathbf{y}_{s_1-k+1}^{k,1} \dots \mathbf{y}_{s_1}^{k,1}} & \underbrace{\square \square \dots \square}_{m_l+m_r} \\
& \swarrow & \searrow \\
\underbrace{\square \square \dots \square}_l & \overline{\mathbf{y}_1^{k,2} \dots \mathbf{y}_{s_2-k}^{k,2} \mathbf{y}_{s_2-k+1}^{k,2} \dots \mathbf{y}_{s_2}^{k,2}} & \underbrace{\square \square \dots \square}_r
\end{array}
\end{array} \tag{3.43}$$

This diagram illustrates symbolically the content of the result (3.40). Again, the first line of this diagram represents the initial condition $\rho_0 = \rho_{\mathbf{x}^1, \mathbf{x}^2}^{(l, m_l, m_r, r)}$. The subsequent lines correspond to the projectors $P_{\mathbf{y}^{1,1}, \mathbf{y}^{1,2}}^{(l, m_l, m_r, r)}, \dots, P_{\mathbf{y}^{k,1}, \mathbf{y}^{k,2}}^{(l, m_l, m_r, r)}$ representing the subsequent propositions of the history $h_{\bar{\mathbf{y}}^1, \bar{\mathbf{y}}^2}$. The coarse-grained islands in the middle of each line, with $m_l + m_r$ empty boxes each, subsequently represent the sums $\sum_{\xi}, \sum_{\eta^1}, \sum_{\eta^2}, \dots, \sum_{\eta^k}$ in our calculation. Again, the step-by-step shift condition is depicted by arrows and lines. Underlined substrings are shifted onto those overlined substrings which are indicated by arrows. In order to fulfil the step-by-step shift condition all underlined and overlined substrings that

are connected by an arrow must be equal. In this way we immediately see which bits of the symbolic specification of a history are completely determined by the initial condition. In the diagram these bits are indicated by using bold face. The remaining bits, which are not in bold face, may be chosen arbitrarily. For instance, in the first iteration step the initial condition substrings $\mathbf{x}_{2:s_1}^1 \equiv x_2^1 \dots x_{s_1-2}^1 x_{s_1-1}^1 x_{s_1}^1$ and $\mathbf{x}_{2:s_2}^2 \equiv x_2^2 \dots x_{s_2-2}^2 x_{s_2-1}^2 x_{s_2}^2$ are shifted onto the substrings $\mathbf{y}_{1:(s_1-1)}^{1,1} \equiv y_1^{1,1} y_2^{1,1} \dots y_{s_1-2}^{1,1} y_{s_1-1}^{1,1}$ and $\mathbf{y}_{1:(s_2-1)}^{1,2} \equiv y_1^{2,2} y_2^{2,2} \dots y_{s_2-2}^{2,2} y_{s_2-1}^{2,2}$, respectively. The first $(s_1 - 1)$ bits of the string $\mathbf{y}^{1,1}$ and the first $(s_2 - 1)$ bits of the string $\mathbf{y}^{1,2}$ of the first event in the history are therefore determined by the initial condition. Unless $\mathbf{y}_{1:(s_1-1)}^{1,1} = \mathbf{x}_{2:s_1}^1$ and $\mathbf{y}_{1:(s_2-1)}^{1,2} = \mathbf{x}_{2:s_2}^2$ is satisfied by the first event the whole history will have vanishing probability. On the other hand the last bits $y_{s_1}^{1,1}$ and $y_{s_2}^{1,2}$ of the strings $\mathbf{y}^{1,1}$ and $\mathbf{y}^{1,2}$, which denote the first event of the history, remain undetermined, because the unspecified bits of the empty boxes are shifted onto them, which are coarse-grained (i.e. summed) over. The bits $y_{s_1}^{1,1}$ and $y_{s_2}^{1,2}$ may therefore be chosen arbitrarily resulting in a branching into four possible histories with non-vanishing probabilities. This procedure repeats with each iteration step of the evolution. The second step leads to a determination of the first $(s_1 - 1)$ bits of the string $\mathbf{y}^{2,1}$ and the first $(s_2 - 1)$ bits of the string $\mathbf{y}^{2,2}$ symbolising the second event of the history, whereas, again, the last bits of these strings remain unspecified and may be chosen arbitrarily implicating a branching into further four alternatives with non-vanishing probabilities. And so on. It becomes clear from the above picture which histories arise with significant probabilities during the evolution and why the number of alternative equiprobable histories is quadruplicated after each iteration step. After k iteration steps—we still assume $k < m_l + m_r$ —there are therefore $2k$ independent bits which can be chosen arbitrarily, given the step-by-step shift constraint. This implicates 2^{2k} alternative, equiprobable histories that may arise with significant probability after k iteration steps.

Our result for $k > m_l + m_r$, Eq. (3.41), may be interpreted in the following way. As long as the number of iterations k is smaller than $m = m_l + m_r$ the number of histories with asymptotically non-vanishing probabilities becomes four times larger after each iteration step of the quantum baker's map resulting in an entropy increase of 2 bits per iteration step. As soon as the number of iterations becomes greater than $m = m_l + m_r$, the entropy increase becomes 1 bit per iteration step. This is what is expressed by the result $2^{-(m_l+m_r)} \cdot 2^{-k} = 2^{-2(m_l+m_r)} \cdot 2^{-(k-(m_l+m_r))}$ for the probability of the histories which are allowed to occur. The first $m_l + m_r$ iteration steps lead to an entropy increase of 2 bits per step involving

$2^{2(m_l+m_r)}$ asymptotically equiprobable histories. The remaining $k - (m_l + m_r)$ iteration steps produce an entropy increase of 1 bit per step only, with the number of histories with significant probabilities being doubled at each step, implicating a branching factor $2^{k-(m_l+m_r)}$. The entire number of histories arising with significant probabilities after k iteration steps therefore becomes $2^{2(m_l+m_r)} \cdot 2^{k-(m_l+m_r)} = 2^{(m_l+m_r)} \cdot 2^k$, the histories being asymptotically equiprobable. Again the issue becomes clearer when using our diagram picture. The size of the middle coarse-grained islands is now only $m_l + m_r < k$. So only in the first m_l+m_r iteration steps coarse-grained bits are shifted onto the last bits of the strings $\mathbf{y}^{j,1}$, making them by this means unspecified, i.e. arbitrarily chose-able for the history. In the subsequent, remaining $k - (m_l + m_r)$ iteration steps the string \mathbf{x}^2 of the initial condition enters the scale of the $\mathbf{y}^{j,1}$ -strings, with the consequence that the last bits of the strings $\mathbf{y}^{m_l+m_r+1,1}, \dots, \mathbf{y}^{k,1}$ become determined by the initial condition. At the end, after the k -th iteration step, only $m_l + m_r$ bits of the string $\mathbf{y}^{k,1}$ may be chosen arbitrarily, the first $s_1 - k$ bits and the last $k - (m_l + m_r)$ bits of it being determined by the initial condition. On the other hand only the first $s_2 - k$ bits of the string $\mathbf{y}^{k,2}$ become determined by the initial condition, whereas all the last k bits of it remain arbitrarily chose-able for the history, provided that $k < r$. This explains the result $2^{(m_l+m_r)} \cdot 2^k$ for the number of alternative histories satisfying the shift constraint. For the entropy of the approximately decoherent set of histories $\{h_{\bar{\mathbf{y}}^1, \bar{\mathbf{y}}^2}\}$ we get the result:

- Entropy after k iteration steps in case $k \geq m_l + m_r$:

$$\begin{aligned} H[\{h_{\bar{\mathbf{y}}^1, \bar{\mathbf{y}}^2}\}] &= - \sum_{\bar{\mathbf{y}}^1, \bar{\mathbf{y}}^2} p[h_{\bar{\mathbf{y}}^1, \bar{\mathbf{y}}^2}] \log_2 p[h_{\bar{\mathbf{y}}^1, \bar{\mathbf{y}}^2}] \\ &= k + (m_l + m_r) + \mathcal{O}\left(\frac{(l+r-k) \log_2(l+r-k)}{2^{l-2(k^2+(1+m_l+m_r)k)}}\right). \end{aligned} \quad (3.44)$$

2. Hierarchical (multi-scale) coarse-grainings

We will see in the following that by introducing more and more scales that are coarse-grained over in the symbolic representation of the dynamics the short-term behaviour of the coarse-grained evolution of the quantum baker's map will exhibit a growing entropy increase per iteration step, i.e., growing unpredictability.

So let us now look at the generalised type of histories (3.19). The evaluation of the corresponding decoherence functional (3.21) is done in a similar way as for the case $\lambda = 2$.

We first state the result for the short-term regime which we now define to be given by $k < \min\{m_1, m_2, \dots, m_{\lambda-1}\}$:

- Decoherence functional in the case $k < \min\{m_1, m_2, \dots, m_{\lambda-1}\}$:

$$\begin{aligned}
\mathcal{D}_{B, \rho_0}[h_{\bar{\mathbf{y}}^1, \bar{\mathbf{y}}^2, \dots, \bar{\mathbf{y}}^\lambda}, h_{\bar{\mathbf{z}}^1, \bar{\mathbf{z}}^2, \dots, \bar{\mathbf{z}}^\lambda}] &= 2^{-\lambda k} \cdot \underbrace{\left(\prod_{j=1}^k \prod_{i=1}^{\lambda} \delta_{\mathbf{y}^{j,i}}^{\mathbf{z}^{j,i}} \right)}_{\text{diagonal}} \cdot \underbrace{\left(\prod_{i=1}^{\lambda} \delta_{\mathbf{y}_{1:s_i-1}}^{\mathbf{x}_{2:s_i}^i} \right)}_{\text{first shift}} \times \\
&\times \underbrace{\left(\prod_{j=1}^{k-1} \prod_{i=1}^{\lambda} \delta_{\mathbf{y}_{1:s_i-1}}^{\mathbf{y}_{j+1,i}^{j,i}} \right)}_{\text{step-by-step shift}} \cdot \underbrace{\left(\prod_{i=1}^{\lambda} \delta_{\mathbf{y}_{1:s_i-k}}^{\mathbf{x}_{k+1:s_i}^i} \right)}_{k\text{-th shift}} \quad (3.45) \\
&+ \mathcal{O}\left(\frac{l+r-k}{2^{l-2(k^2+(1+m_1+m_2+\dots+m_{\lambda-1})k)}}\right).
\end{aligned}$$

In the limit of large l the off-diagonal elements of the decoherence functional vanish and the set of histories becomes decoherent. The diagonal elements of the functional may therefore be interpreted as probabilities. The coarse-grained evolution is again governed by shift constraints. Only such histories are allowed to arise with significant probabilities that satisfy the shift condition, which has been illustrated in detail for the case $\lambda = 2$ above. Here we are mainly interested in the rate of the entropy increase. The result (3.45) shows that in the short-term regime, i.e. as long as $k < \min\{m_1, m_2, \dots, m_{\lambda-1}\}$, the coarse-grained evolution exhibits an entropy increase of λ bits per iteration step, provided that l is very large (classical limit). This is quantitatively expressed by the entropy of the approximately decoherent set of histories:

- Entropy after k iteration steps in case $k < \min\{m_1, m_2, \dots, m_{\lambda-1}\}$:

$$\begin{aligned}
H[\{h_{\bar{\mathbf{y}}^1, \bar{\mathbf{y}}^2, \dots, \bar{\mathbf{y}}^\lambda}\}] &= - \sum_{\bar{\mathbf{y}}^1, \bar{\mathbf{y}}^2, \dots, \bar{\mathbf{y}}^\lambda} p[h_{\bar{\mathbf{y}}^1, \bar{\mathbf{y}}^2, \dots, \bar{\mathbf{y}}^\lambda}] \log_2 p[h_{\bar{\mathbf{y}}^1, \bar{\mathbf{y}}^2, \dots, \bar{\mathbf{y}}^\lambda}] \\
&= \lambda \cdot k + \mathcal{O}\left(\frac{(l+r-k) \log_2(l+r-k)}{2^{l-2(k^2+(1+m_1+m_2+\dots+m_{\lambda-1})k)}}\right), \quad (3.46)
\end{aligned}$$

where we used $p[h_{\bar{\mathbf{y}}^1, \bar{\mathbf{y}}^2, \dots, \bar{\mathbf{y}}^\lambda}] = \mathcal{D}_{B, \rho_0}[h_{\bar{\mathbf{y}}^1, \bar{\mathbf{y}}^2, \dots, \bar{\mathbf{y}}^\lambda}, h_{\bar{\mathbf{y}}^1, \bar{\mathbf{y}}^2, \dots, \bar{\mathbf{y}}^\lambda}]$.

For the long-term regime, which we define by $k > \max\{m_1, \dots, m_{\lambda-1}\}$, our analysis yields the following results:

- Decoherence functional in case $k > \max\{m_1, m_2, \dots, m_{\lambda-1}\}$:

$$\mathcal{D}_{B, \rho_0}[h_{\bar{\mathbf{y}}^1, \bar{\mathbf{y}}^2, \dots, \bar{\mathbf{y}}^\lambda}, h_{\bar{\mathbf{z}}^1, \bar{\mathbf{z}}^2, \dots, \bar{\mathbf{z}}^\lambda}] =$$

$$\begin{aligned}
&= 2^{-k-(m_1+\dots+m_{\lambda-1})} \cdot \underbrace{\left(\prod_{j=1}^k \prod_{i=1}^{\lambda} \delta_{\mathbf{y}^{j,i}}^{z^{j,i}} \right)}_{\text{diagonal}} \cdot \underbrace{\left(\prod_{i=1}^{\lambda} \delta_{\mathbf{y}_{1:s_i-1}^{x_{2:s_i}^i}} \right)}_{\text{first shift}} \times \\
&\quad \times \underbrace{\left(\prod_{j=1}^{k-1} \prod_{i=1}^{\lambda} \delta_{\mathbf{y}_{1:s_i-1}^{j+1,i}}^{j,i} \right)}_{\text{step-by-step shift}} \cdot \underbrace{\left(\prod_{i=1}^{\lambda} \delta_{\mathbf{y}_{1:s_i-k}^{x_{k+1:s_i}^i}} \right)}_{k\text{-th shift}} \quad (3.47) \\
&+ \mathcal{O}\left(\frac{l+r-k}{2^{l-2(k^2+(1+m_1+m_2+\dots+m_{\lambda-1})k)}}\right)
\end{aligned}$$

- Entropy after k iteration steps in case $k > \max\{m_1, m_2, \dots, m_{\lambda-1}\}$:

$$H[\{h_{\bar{\mathbf{y}}^1, \bar{\mathbf{y}}^2, \dots, \bar{\mathbf{y}}^\lambda}\}] = k + \sum_{i=1}^{\lambda-1} m_i + \mathcal{O}\left(\frac{(l+r-k) \log_2(l+r-k)}{2^{l-2(k^2+(1+m_1+m_2+\dots+m_{\lambda-1})k)}}\right). \quad (3.48)$$

The interpretation of these results is similar to the special case $\lambda = 2$ of the last section. Whereas in the short-term regime, $k < \min\{m_1, \dots, m_{\lambda-1}\}$, the entropy production rate is λ bits per iteration, in the long-term regime $k > \max\{m_1, \dots, m_{\lambda-1}\}$, the entropy production drops to 1 bit per iteration, independently of the values of the parameters $m_1, \dots, m_{\lambda-1}$, which determine the border between the regimes. In the intermediate regime, the entropy production rate decreases each time k exceeds one of the values $m_1, \dots, m_{\lambda-1}$.

Acknowledgments

We would like to thank Todd Brun for helpful discussions. This work was supported in part by the European Union IST-FET project EDIQIP.

-
- [1] M. Gell-Mann and J. B. Hartle, Phys. Rev. D **47**, 3345 (1993).
 - [2] T. A. Brun and J. B. Hartle, Phys. Rev. D **60**, 123503 (1999).
 - [3] R. Griffiths, J. Stat. Phys. **36**, 219 (1984).
 - [4] R. Omnès, J. Stat. Phys. **53**, 893, 933, 957 (1988).
 - [5] M. Gell-Mann and J. B. Hartle, in *Complexity, Entropy, and the Physics of Information*, edited by W. H. Zurek (Addison Wesley, Redwood City, CA, 1990).
 - [6] H. F. Dowker and J. J. Halliwell, Phys. Rev. D **46**, 1580 (1992).

- [7] N. L. Balazs and A. Voros, *Ann. Phys.* **190**, 1 (1989).
- [8] M. Saraceno, *Ann. Phys.* **199**, 37 (1990).
- [9] V. I. Arnold and A. Avez, *Ergodic Problems of Classical Mechanics* (Benjamin, New York, 1968).
- [10] M. V. Berry, N. L. Balazs, M. Tabor, and A. Voros, *Ann. Phys.* **122**, 26 (1979).
- [11] H. Weyl, *The Theory of Groups and Quantum Mechanics* (Dover, New York, 1950).
- [12] R. Schack and C. M. Caves, *Applicable Algebra in Engineering, Communication and Computing (AAECC)* **10**, 305 (2000).
- [13] V. M. Alekseev and M. V. Yakobson, *Phys. Reports* **75**, 287 (1981).
- [14] A. N. Soklakov and R. Schack, *Phys. Rev. E* **61**, 5108 (2000).
- [15] J. B. Hartle, *Physica Scripta* **T76**, 67 (1998).
- [16] T. A. Brun and J. B. Hartle, *Phys. Rev. E* **59**, 6370 (1999).
- [17] T. A. Brun, *Phys. Lett. A* **206**, 167 (1995).
- [18] A. Scherer and A. N. Soklakov, *J. Math. Phys.* **46**, 042108 (2005).
- [19] A. N. Soklakov and R. Schack, *Phys. Rev. E* **66**, 036212 (2002).
- [20] The support of a Hermitian operator A is defined to be the vector space spanned by the eigenvectors of A corresponding to its non-zero eigenvalues.